# Cross-bispectrum Computation and Variance Estimation


K. S. LII*

University of California, Riverside

K. N. HELLAND**

University of California, San Diego

Abstract

A method for the estimation of cross-bispectra of discrete real time series is developed. The asymptotic variance properties of the bispectrum are reviewed, and a method for the direct estimation of bispectral variance is given. The symmetry properties are described which minimize the computations necessary to obtain a complete estimate of the cross-bispectrum in the right-half-plane. A procedure is given for computing the cross-bispectrum by subdividing the domain into rectangular averaging regions which help reduce the variance of the estimates and allow easy application of the symmetry relationships to minimize the computational effort. As an example of the procedure, the cross-bispectrum of a numerically generated, exponentially distributed time series is computed and compared with theory.

---

* Author's address: Department of Statistics, University of California, Riverside, CA 92521.

** Author's address: Department of Applied Mechanics and Engineering Sciences, University of California, San Diego, La Jolla, CA 92093.

## 1. Introduction

Bispectral analysis is currently experiencing a degree of popularity with applications in a number of diverse fields. The bispectrum was originally proposed by Hasselman, Munk & MacDonald [1] as a statistical tool for investigating nonlinear interacting ocean waves, and Godfrey [2] used the bispectrum for analyzing economic time series. The statistical properties of bispectral estimation and variance were reported by Brillinger & Rosenblatt [3] and included an application to the analysis of sunspots. Large sample theoretical investigations of bispectral estimates are described in Brillinger & Rosenblatt [4]. Huber et al. [5] used bispectra to investigate EEG readings, and Roden & Bendliner [6] used cross-bispectra to study profiles of oceanographic variables such as density and salinity. Various aspects of spectral energy transfer in laboratory and atmospheric turbulence have been studied using bispectral and cross-bispectral techniques by Lii, Rosenblatt & Van Atta [7], by Helland, Lii & Rosenblatt [8, 9], and by Van Atta [10, 11]. Sato & Sasaki [12] used bispectral methods to eliminate additive Gaussian noises in the reading of laser holograms. A real-time bispectral technique developed by Sato, Sasaki & Nakamura [13] was used to analyze noise in mechanical gear trains. Kim & Powers [14] have shown that a bispectral analysis is useful in distinguishing between spontaneously excited modes and coupled modes in plasma wave studies, and McComas [15] has reported on theoretical and experimental bispectra calculations for studies of internal waves in the ocean.

The purpose of the present study is to review the bias and variance properties of the bispectrum, and consider the practical estimation problem of the

general cross-bispectrum for a multivariate time series. The computational simplifications which result when the bispectral analysis involves only one or two separate time series are reviewed. A FORTRAN subroutine which implements these considerations is discussed and a listing of the algorithm is available from the authors.

## 2. Theory

We are to estimate the cross-spectrum of three stationary real-valued time series defined by $X_1(i), X_2(i), X_3(i)$; $i = 0, \ldots, T-1$ with zero mean. Detailed asymptotic results of the k-th order spectra can be found in [3].

For computational purposes we define the discrete Fourier transform

$$F_j(\lambda) = \sum_{t=0}^{T-1} X_j(t) \exp\{-i\lambda t\} \quad , \quad j = 1, 2, 3 \tag{2.1}$$

and the bispectral periodogram

$$B_{1,2,3}(\lambda_1, \lambda_2, \lambda_3) = \frac{1}{(2\pi)^2 T} \prod_{j=1}^{3} F_j(\lambda_j) \tag{2.2}$$

where

$$\sum_{j=1}^{3} \lambda_j = 0 \ (\text{modulo } 2\pi)$$

$$\lambda_j = \frac{2\pi s_j}{T} \quad \text{with } s_j \text{ integers.}$$

If the mean is not removed before taking the Fourier transform, then set $F_j(0) = 0$. Now taking the average or expected value of the periodogram

$$E B_{1,2,3}(\lambda_1, \lambda_2, \lambda_3) \cong b(\lambda_1, \lambda_2) \tag{2.3}$$

where $b(\lambda_1, \lambda_2)$ is the cross-bispectrum of the joint cumulant of $X_i$, $i = 1, 2, 3$, and E is the expectation operator. Also the asymptotic variance estimate [4] is given by

$$\left.\begin{matrix} \mathrm{Var}(\mathrm{Re}\, B_{1,2,3}(\lambda_1, \lambda_2, \lambda_3)) \\ \mathrm{Var}(\mathrm{Im}\, B_{1,2,3}(\lambda_1, \lambda_2, \lambda_3)) \end{matrix}\right\} \cong \frac{T}{4\pi} f_1(\lambda_1) f_2(\lambda_2) f_3(\lambda_1 + \lambda_2) \tag{2.4}$$

where $f_i(\lambda)$ is the power spectrum of $X_i$. The asymptotic covariance between the real and imaginary parts is an order of magnitude smaller, as is the covariance between different frequencies. To reduce the variance of an estimate we can average $B_{1,2,3}(\lambda_1, \lambda_2)$ from disjoint time blocks (i.e. partition a long stretch of data into disjoint segments or records of equal length) and smooth spatially (over frequencies). The spatial smoothing should not be too broad otherwise the bias of the estimate would become large. When the bispectrum is relatively smooth, the smoothing window shape is not critical. For most purposes, the uniform window is adequate and greatly simplifies the computation. In the course of computation, it is important to compute an estimate of the standard deviation of the bispectrum. If we have m records of data and n points being averaged in the frequency domain, then the estimated standard deviation (S. D.) at $(\lambda_1, \lambda_2)$ for the real part is

$$\text{S. D.}(\lambda_1, \lambda_2) = \left[\frac{1}{m} \text{ VAR Re } B(\lambda_1, \lambda_2)\right]^{1/2} \tag{2.5}$$

where

$$\text{VAR Re } B(\lambda_1, \lambda_2) = \frac{1}{m} \sum_{i}^{m} [\text{Re } \bar{B}_i(\lambda_1, \lambda_2) - \text{Re } \bar{\bar{B}}(\lambda_1, \lambda_2)]^2 \tag{2.6}$$

with

$$\bar{B}_i(\lambda_1, \lambda_2) = \frac{1}{n} \sum_{j=1}^{n} B_{1,2,3}(\lambda_1^{(j)}, \lambda_2^{(j)}, \lambda_3^{(j)})$$

$$\bar{\bar{B}}(\lambda_1, \lambda_2) = \frac{1}{m} \sum_{i=1}^{m} \bar{B}_i(\lambda_1, \lambda_2) \quad .$$

The standard deviation of the imaginary part, Im B, of our estimates is computed by the analogous method. These estimated standard deviations give us a picture of the relative resolvability of bispectrum at each frequency pair $(\lambda_1, \lambda_2)$ and can be compared with that of asymptotic variance in Eq. (2.4).

The asymptotic formula Eq. (2.4) for the variance can serve a fundamental role during the design of an experiment. The power spectra, $f_i(\lambda)$, are often available or are readily estimated from preliminary data. The asymptotic variance formula and preliminary computations of the bispectrum should then be used to determine important experimental parameters such as duration of the data, number of records, and size of the spatial averaging required to obtain a desired degree of statistical resolution in the final bispectral estimate. The directly estimated standard deviation given in Eq. (2.5) should be used to verify that the degree of statistical resolution has actually been obtained from the data analysis.

## 3. Symmetries

The basic symmetry of the cross-bispectrum of real time series is obtained by conjugation

$$b(\lambda_1, \lambda_2) = b^*(-\lambda_1, -\lambda_2) \qquad (3.1)$$

where $b^*$ is the complex conjugate of b. Thus, we need only compute the right half-plane of Figure 1. When dealing with a single time series, i.e., $X_1 = X_2 = X_3$, then by various symmetries we only need to compute region 2. All other regions can be computed from region 2 using the relationships in Table 1. When $X_2 = X_3 = Y$, then since

$$b_{XYY}(\lambda_1, \lambda_2, -\lambda-\lambda_2) = b_{XYY}(\lambda_1, -\lambda_1-\lambda_2, \lambda_2) \tag{3.2}$$

we only need to compute regions 1-3. Regions 4, 5, 6 are obtained from regions 3, 2, 1, respectively, using Eq. (3.2) in the appropriate region.

Note that all these computations should be made away from $\lambda_i = 0$ to avoid introducing a severe bias in the bispectral estimates in the neighborhood of $\lambda_i = 0$. If estimates are needed at a point $B(\lambda_1, \lambda_2, \lambda_3)$ involving some $\lambda_i = 0$ then interpolation via a continuity assumption or other methods should be made.

## 4. Computational Methods

The fundamental computation required for bispectral estimates is given by Eq. (2.2), the triple complex product of the three individual Fourier transforms. While this computation is straightforward, limitations on computer time, memory, and statistical variance impose severe limitations on implementation of the definition of the bispectrum. If record lengths are short, then it is a simple matter to compute the triple complex products at each pair of frequencies in the right-half-plane. Applications of bispectral analyses usually involve long records, and spatial averaging is often required in order to reduce the variance of the bispectral estimates.

Increasing the number of records is demanding on computer time and introduces potential nonstationarities. The spatial averaging can be implemented by summing over triple products in a neighborhood of a frequency pair $(\lambda_1, \lambda_2)$. The summation must be performed record-by-record because the number of frequency pairs is large even for moderate record lengths. Computation of a large number of bispectral estimates is time consuming even on large mainframe computers, and it is therefore desirable to compute the estimates over an arbitrary set of subregions in the right-half-plane. This approach permits taking full advantage of the symmetry relationships discussed in Section 3.

In the proposed algorithm the bispectral estimates are computed by averaging over rectangular regions which may be located anywhere in the right-half-plane and bounded by the Nyquist frequency constraint imposed by the discrete Fourier transform. The rectangular regions may be reduced to a single point if the variance properties of the data justify the sharp resolution. Coordinates for the averaging rectangles are passed to the subroutine and the location of the rectangles is arbitrary. This permits easy computation of the bispectrum for selected regions when strong interactions are expected for isolated frequency combinations. The bispectrum and variance estimates are indexed by the averaging rectangle. The bispectrum computation is divided into a number of subregions which depend on the location of the averaging rectangle. This is done to eliminate most of the conditional tests from the inner loops thereby substantially improving the computational efficiency. The algorithm requires that the Fourier transform be defined out to twice the Nyquist frequency index in order to eliminate

conditional tests in the first quadrant. Some discrete Fourier transform algorithms already contain this symmetrical part and the user is responsible for the existence of the extension. A sample computation to extend the transform beyond the Nyquist frequency is included in the comments of the bispectral algorithm.

In the first quadrant the bispectral estimate at a point is given by

$$B(i, j) = F_1(i)\, F_2(j)\, F_3(k) \tag{4.1}$$

where $i + j + k = 0$, or $k = -(i + j)$. Note that the range of indices i, j, and k are assumed to contain 0 and the scale factor $1/(2\pi)^2 T$ has been surpressed; the Fortran implementation incorporates a shift by one to avoid the zero index. The Hermitian property of the Fourier transform of a real time series implies that

$$F_3(k) = F_3^*(-k) \tag{4.2}$$

and thus the bispectral estimate in the first quadrant becomes

$$B(i, j) = F_1(i)\, F_2(j)\, F_3^*(-k) \ . \tag{4.3}$$

As shown in Section 3 bispectral estimates do not need to be made in the second and third quadrants. In the fourth quadrant $i > 0$, $j < 0$, and k may be either positive or negative. The dividing line is $i = -j$. Thus depending on the relative magnitudes of i and j, the expression for the bispectral estimates becomes: For $k < 0$,

$$B(i, j) = F_1(i)\, F_2^*(-j)\, F_3^*(-k) \ , \tag{4.4}$$

and for $k > 0$,

$$B(i, j) = F_1(i)\, F_2^*(-j)\, F_3(k) \ . \tag{4.5}$$

In the implementation of these considerations, there is a strip along $i = -j$ where $k$ may be of either sign; this is a result of the finite size of the averaging rectangles. In the algorithm, the fourth quadrant is divided into three separate computation loops, one with $k > 0$, one with $k < 0$, and a third with $k$ taking on positive and negative values. The point-wise conditional test remains in this third loop but not in the first and second loops. We feel that the small loss of efficiency of including the conditional test to select Eq. (4.4) or (4.5) in the third loop is worth the simplification gained over eliminating even more of the required conditional tests. In a global bispectrum computation only a small percentage of the loops will actually include the point-wise conditional test.

The algorithm does not perform the final scaling for the number of records used in the bispectral computation, the conversion to physical units or the $1/(2\pi)^2 T$ factor in Eq. (2.2). The final scaling depends on the particular implementation of the discrete Fourier transform used in the computation.

## 5. Application

The proposed method for computation of bispectra is applied to an exponentially distributed process. Let $X_1(i)$, $i = 1, \ldots, N$ be independent, identically distributed time series with $X(i)$ exponentially distributed with parameter $\alpha$. Then $X(i)$ has a probability function $P(X) = \frac{1}{\alpha} \exp\{-X/\alpha\}$, $X \geq 0$, and the $k^{th}$ cumulant of $X(i)$ is $C_k = (k-1)!\, \alpha^k$. Consider two useful test cases:

(1) If $X_1(i) = X_2(i) = X_3(i)$ then

$$b_{X_1, X_1, X_1}(\lambda_1, \lambda_2, \lambda_3) = \frac{1}{(2\pi)^2} C_3, \quad \Sigma\lambda_i = 0 \text{ (modulo } 2\pi) ; \qquad (5.1)$$

(2) If $X_2(i) = \frac{1}{M} \sum_{j=-\ell}^{\ell} X_1(i+j)$, application of the running mean (5.2)

filter to the exponential process with $\ell = (M-1)/2$ integer and $X_3 = X_1$

$$b_{X_1, X_2, X_1}(\lambda_1, \lambda_2) = \frac{C_3}{(2\pi)^2} \frac{\text{Sin}(\lambda_2 M/2)}{M \text{ Sin}(\lambda_2/2)} \qquad (5.3)$$

for $-\pi < \lambda_2 \leq \pi$. The power spectrum for signal $X_1$ and $X_2$ are

$$f_{X_1}(\lambda) = \frac{1}{2\pi} C_2 \text{ , for all } \lambda \text{ ,} \qquad (5.4)$$

and

$$f_{X_2}(\lambda) = \frac{1}{2\pi} \left[\frac{\text{Sin}(\lambda M/2)}{M \text{ Sin}(\lambda/2)}\right]^2 \qquad (5.5)$$

respectively.

From Eqs. (5.4) and (5.5) for the power spectra of $X_1$ and $X_2$ the theoretical variance of the estimates are calculated from Eq. (2.4) to give

$$\text{VAR}(b_{X_1, X_2, X_3}) = \frac{T}{32\pi^4} C_2^3 \qquad (5.6)$$

for case 1 and

$$\text{VAR}(b_{X_1, X_2, X_1}) = \frac{T}{32\pi^4} C_2^2 \left[\frac{\text{Sin}(\lambda M/2)}{M \text{ Sin}(\lambda/2)}\right]^2 \qquad (5.7)$$

for case 2.

While both cases have been tested, we choose to report on the second case because the cross-bispectrum exercises all the loops of the algorithm. Case 1 is useful for checking the simple bispectrum computation, but does not involve all the possible loops. Case 2 was implemented in a test program and the cross-bispectrum was computed using the method described in Section 4. The parameters chosen are the transform length $T = 256$, the number of points included in the averaging rectangle $n = 11 \times 11 = 121$, and the number of records $m = 100$. In addition, M in Eq. (5.2) is chosen to be 5, and the exponential process parameter $\alpha = 1$. The time series was generated and discrete Fourier transformed using standard IMSL subroutines. The numerical estimates for the real and imaginary parts of the cross-bispectrum together with the standard deviation of the estimates are given in Tables 2 and 3, respectively. An extra column is included in Tables 2 and 3 giving the theoretical values for the real and imaginary parts of the cross-bispectrum and the theoretical standard deviations. A single column is sufficient since the theoretical values given in Eqs. (5.3) and (5.7) are constant for $\lambda_2 = \text{constant}$. The cross-bispectrum was computed in regions 1-3 of Fig. 1(a) and Fig. 1(c). These results are shown in Fig. 2.

Table 2 shows that the real part of the estimated cross-bispectrum is an order of magnitude larger than the estimated standard deviation, and the result is considered to be well resolved. Table 3 shows that the estimated imaginary part is effectively zero since it is comparable to or smaller than the estimated standard deviation. A comparison of estimated and theoretical values for the real part in Table 2 shows that the differences are small relative to the standard deviation whereas the estimated and theoretical standard

deviations are comparable. The comparison between numerical and theoretical cross-bispectra has been statistical in nature and clearly exact agreement should not be expected. The accuracy of the algorithm was tested by a deterministic sine-cosine signal, as well as the application just discussed. The comparison obtained between the numerical and theoretical cross-bispectra provide strong support for the accuracy of the algorithm in estimating both the mean and standard deviation of bispectra and cross-bispectra.

## 6. Concluding Remarks

We have described a method for computing the bispectral and cross-bispectral estimates of up to three separate time series at any point in the right-half-plane. Proper application of the algorithm involves:

(i) The computational domain must be chosen to minimize the computation time required by observing the symmetry relationships.

(ii) The averaging rectangles should be of optimum size to both keep the ratio of mean to standard deviation as large as possible without making the rectangles so large as to lose the spatial (frequency) resolution of important features in a particular application. If there is no theoretical guidance available in a particular application, then the user must proceed in a trial-and error technique to find the optimum computational parameters.

A source listing of the computer subroutine which implements the proposed method is available from the authors.

Acknowledgments

The authors wish to thank Professor M. Rosenblatt and Mr. R. A. Stanford for helpful discussions. This work was supported by NASA Grant NSG 2376. KNH was partially supported by National Science Foundation Grant ENG78-25080.

## References


1. Hasselmann, K., Munk, W., and MacDonald, G. Bispectra of Ocean Waves. In Time Series Analysis (ed. M. Rosenblatt)(1963), Wiley, 125-139.

2. Godfrey, M. D. An exploratory study of the bispectrum of economic time series. Appl. Statist. (London) 14 (1965), 48-69.

3. Brillinger, D. R., and Rosenblatt, M. Computation and Interpretation of kth order spectra. In Spectral Analysis of Time Series (ed. B. Harris) (1967a), Wiley, 189-232.

4. Brillinger, D. R., and Rosenblatt, M. Asymptotic theory of estimates of kth order spectra. In Spectral Analysis of Time Series (ed. B. Harris) (1967b), Wiley,

5. Huber, P. J., Kleiner, B., Gasser, Th., and Dumermuth, G. Statistical methods for investigating phase relations in stationary stochastic processes. IEEE Trans. Audio Electroacoust. 19 (1971), 78-86.

6. Roden, G. I., and Bendiner, D. J. Bispectra and cross-bispectra of temperature, salinity, sound velocity and density fluctuations with depth off Northeastern Japan, J. Phys. Ocean 3, 3 (1973), 308-317.

7. Lii, K. S., Rosenblatt, M., and Van Atta, C. W. Bispectral measurements in turbulence. J. Fluid Mech. 77, 1 (1976), 45-62.

8. Helland, K. N., Lii, K. S., and Rosenblatt, M. Bispectra of atmospheric and wind tunnel turbulence. In Applications of Statistics (ed. P. R. Krishnaiah) (1977), North-Holland Pub., 223-248.

9. Helland, K. N., Lii, K. S., and Rosenblatt, M. Bispectra and energy transfer in grid-generated turbulence. In Development in Statistics (ed. P. R. Krishnaiah) 2 (1979), 123-155.

10. Van Atta, C. W. Bispectral measurements in turbulence computations. Proc. 6th International Conference on Numerical Methods in Fluid Dynamics. In Lecture Notes in Physics (1978), Springer-Verlag, 530-536.

11. Van Atta, C. W. Inertial range bispectra in turbulence. Phys. Fluids 22, 8 (1979), 1440-1442.

12. Sato, T., and Sasaki, K. Bispectral holography. J. Acoust. Soc. Am. 62, 2 (1977), 404-408.

13. Sato, T., Sasaki, K., and Nakamura, Y. Real-time bispectral analysis of gear noise and its application to contactless diagnosis. J. Acoust. Soc. Am. 62, 2 (1977), 382-387.

14. Kim, Y. C., and Powers, E. J. Digital bispectral analysis of self-excited fluctuation spectra. Phys. Fluids 21, 8 (1978), 1452-1453.

15. McComas, C. H. Bispectra of internal waves. Woods Hole Technical Note 02543 (1978), Woods Hole, Mass.

Table 1. Bispectral symmetries

| $b(\lambda_1, \lambda_2)$ in | Corresponding bispectral coordinates in Region 2 |
|---|---|
| Region 1 | $b(\lambda_2, \lambda_1)$ |
| 3 | $b^*(\lambda_1 + \lambda_2, -\lambda_2)$ |
| 4 | $b^*(-\lambda_2, \lambda_1 + \lambda_2)$ |
| 5 | $b(\lambda_1, -\lambda_1 - \lambda_2)$ |
| 6 | $b(-\lambda_1 - \lambda_2, \lambda_1)$ |

Table 2. Mean and standard deviation of Re $\{B_{121}(\lambda_1, \lambda_2)\}$. The standard deviations are the second entry of each pair.

| | Estimated | | | | | Theory |
|---|---|---|---|---|---|---|
| $\lambda_2$ \ $\lambda_1$ | 0.209 | 0.479 | 0.749 | 1.019 | 1.289 | |
| 1.289 | .1442E-02 | .1774E-02 | .1289E-02 | .1542E-02 | .1647E-02 | .1676E-02 |
| | .2226E-03 | .2697E-03 | .1980E-03 | .2163E-03 | .2415E-03 | .8618E-04 |
| 1.019 | -.1016E-01 | -.1036E-01 | -.9699E-02 | -.1033E-01 | -.1077E-01 | -.1105E-01 |
| | .8683E-03 | .9787E-03 | .8137E-03 | .1362E-02 | .8895E-03 | .5683E-03 |
| 0.884 | -.1278E-01 | -.1284E-01 | -.1241E-01 | -.1366E-01 | -.1350E-01 | -.1254E-01 |
| | .1175E-02 | .1231E-02 | .9390E-03 | .1105E-02 | .1237E-02 | .6450E-03 |
| 0.614 | .1382E-02 | .1646E-02 | .1139E-02 | .1410E-02 | .1625E-02 | .1294E-02 |
| | .2804E-03 | .3197E-03 | .2523E-03 | .3310E-03 | .3336E-03 | .6657E-04 |
| 0.344 | .2973E-01 | .2953E-01 | .2843E-01 | .2982E-01 | .2895E-01 | .2975E-01 |
| | .2223E-02 | .2449E-02 | .2255E-02 | .2345E-02 | .2442E-02 | .1530E-02 |
| 0.074 | .5135E-01 | .5483E-01 | .4518E-01 | .4902E-01 | .4902E-01 | .4957E-01 |
| | .3895E-02 | .4814E-02 | .3307E-02 | .4604E-02 | .5317E-02 | .2549E-02 |
| -0.221 | .3877E-01 | .4394E-01 | .3994E-01 | .4442E-01 | .3734E-01 | .4131E-01 |
| | .3807E-02 | .3718E-02 | .2980E-02 | .3272E-02 | .3599E-02 | .2124E-02 |
| -0.491 | 0. | .1384E-01 | .1300E-01 | .1520E-01 | .1420E-01 | .1364E-01 |
| | 0. | .1592E-02 | .1093E-02 | .1422E-02 | .1298E-02 | .7012E-03 |
| -0.761 | 0. | 0. | -.7440E-02 | -.9131E-02 | -.8540E-02 | -.9040E-02 |
| | 0. | 0. | .6795E-03 | .6603E-03 | .7508E-03 | .4649E-03 |
| -1.031 | 0. | 0. | 0. | -.9039E-02 | -.1033E-01 | -.1068E-01 |
| | 0. | 0. | 0. | .9301E-03 | .9235E-03 | .5492E-03 |
| -1.301 | 0. | 0. | 0. | 0. | .2157E-02 | .2303E-02 |
| | 0. | 0. | 0. | 0. | .2483E-03 | .1185E-03 |

Table 3. Mean and standard deviation of $\mathrm{Im}\{B_{121}(\lambda_1, \lambda_2)\}$. The standard deviations are the second entry of each pair.

| | Estimated | | | | | Theory |
|---|---|---|---|---|---|---|
| $\lambda_2$ \ $\lambda_1$ | 0.209 | 0.479 | 0.749 | 1.019 | 1.289 | |
| 1.289 | .6454E-04 | .1550E-03 | .8761E-04 | .2077E-03 | .6328E-04 | 0 |
| | .1667E-03 | .2108E-03 | .1949E-03 | .1928E-03 | .1833E-03 | .8618E-04 |
| 1.019 | .9291E-03 | .3264E-03 | -.1914E-03 | -.5656E-03 | -.6598E-03 | |
| | .6227E-03 | .6321E-03 | .5889E-03 | .1110E-02 | .6453E-03 | .5683E-03 |
| 0.884 | .7749E-03 | -.1432E-02 | -.5100E-03 | -.1389E-03 | -.5468E-04 | 0 |
| | .5708E-03 | .8008E-03 | .6992E-03 | .7612E-03 | .8250E-03 | .6450E-03 |
| 0.614 | .3441E-03 | -.7569E-04 | -.3259E-03 | -.2345E-03 | .4406E-03 | 0 |
| | .2351E-03 | .2791E-03 | .2762E-03 | .2377E-03 | .3167E-03 | .6657E-04 |
| 0.344 | -.3163E-02 | .3950E-03 | -.3564E-04 | -.1059E-02 | .6072E-03 | 0 |
| | .1578E-02 | .1731E-02 | .1650E-02 | .1727E-02 | .1666E-02 | .1530E-02 |
| 0.074 | -.1008E-02 | .2482E-02 | -.8030E-03 | .7404E-03 | -.7873E-03 | 0 |
| | .2282E-02 | .2496E-02 | .2477E-02 | .2797E-02 | .2328E-02 | .2549E-02 |
| -0.221 | .5043E-03 | .5318E-02 | -.2506E-02 | .2926E-02 | .1942E-02 | 0 |
| | .8090E-03 | .3122E-02 | .2203E-02 | .2298E-02 | .2029E-02 | .2124E-02 |
| 0.491 | 0. | .2691E-03 | -.7447E-04 | -.1566E-02 | -.6623E-03 | 0 |
| | 0. | .3065E-03 | .8888E-03 | .8593E-03 | .9142E-03 | .7012E-03 |
| -0.761 | 0. | 0. | .2005E-03 | -.3593E-03 | .3708E-04 | 0 |
| | 0. | 0. | .2287E-03 | .5141E-03 | .6059E-03 | .4649E-03 |
| -1.031 | 0. | 0. | 0. | -.3671E-03 | -.1164E-02 | 0 |
| | 0. | 0. | 0. | .2665E-03 | .6362E-03 | .5492E-03 |
| -1.301 | 0. | 0. | 0. | 0. | .2579E-03 | 0 |
| | 0. | 0. | 0. | 0. | .1208E-03 | .1185E-03 |

## Figure Captions

Fig. 1 Bispectral domains for discretely sampled data:

(a) $\lambda_1 + \lambda_2 + \lambda_3 = 0$; (b) $\lambda_1 + \lambda_2 + \lambda_3 = -2\pi$;

(c) $\lambda_1 + \lambda_2 + \lambda_3 = 2\pi$.

Fig. 2 Comparison of estimated and theoretical cross-bispectra.

(a) Theoretical real part; (b) estimated real part;

(c) estimated imaginary part.

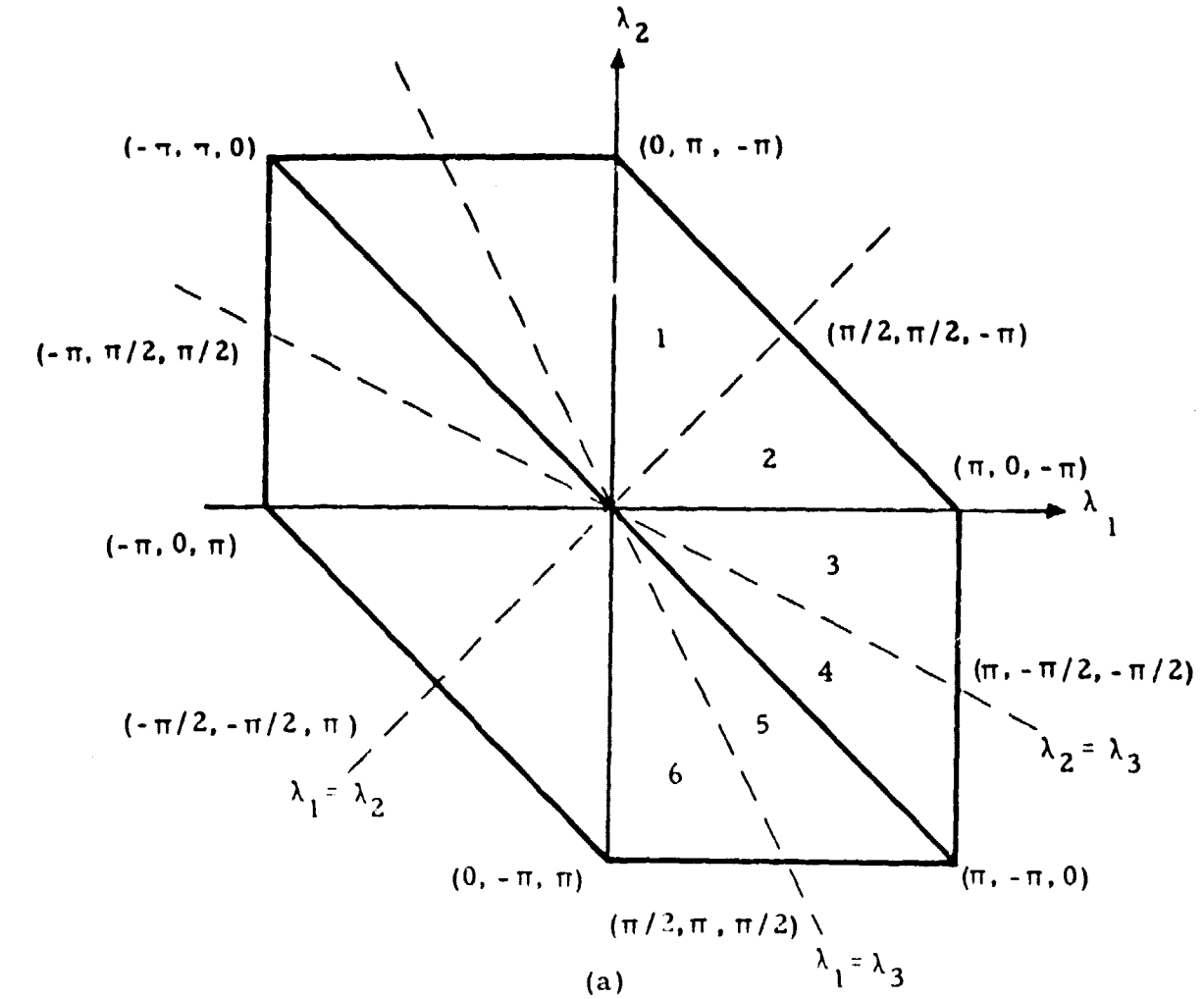
λ2
(-π, π, 0)
(0, π, -π)
(-π, π/2, π/2)
(π/2, π/2, -π)
1
2
(π, 0, -π)
λ1
(-π, 0, π)
3
4
(π, -π/2, -π/2)
(-π/2, -π/2, π)
5
λ2 = λ3
λ1 = λ2
6
(0, -π, π)
(π, -π, 0)
(π/2, π, π/2)
λ1 = λ3

(a)

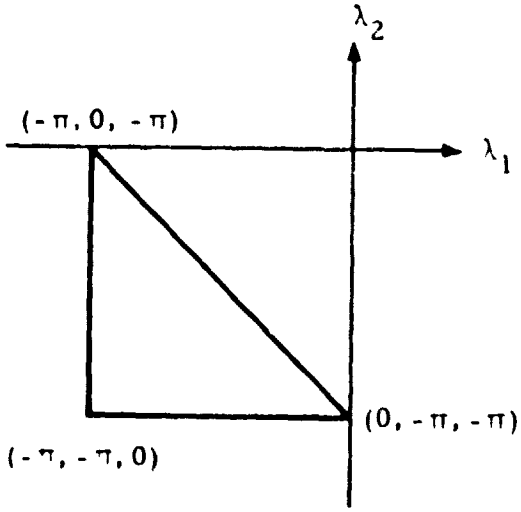
λ2
(-π, 0, -π)
λ1
(0, -π, -π)
(-π, -π, 0)

(b)

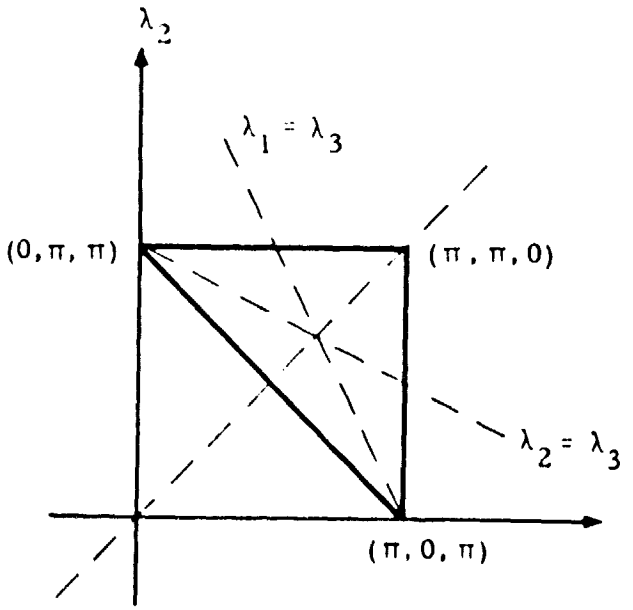
λ2
λ1 = λ3
(0, π, π)
(π, π, 0)
λ2 = λ3
(π, 0, π)

(c)

Fig. 1

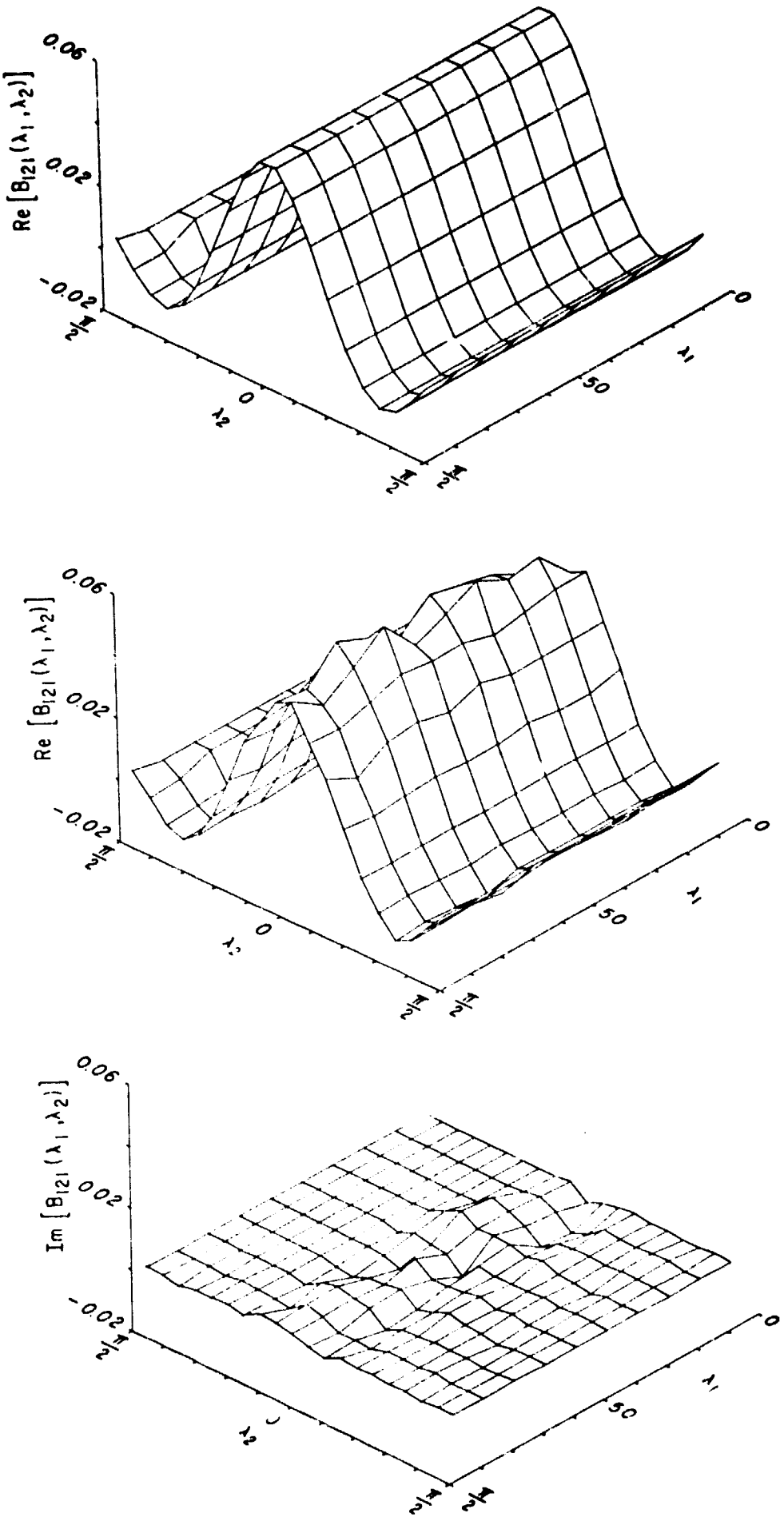
Re [B121 (λ1, λ2)]
0.06
0.02
-0.02
-π/4
0
π/4
λ2
0
50
λ1
Re [B121 (λ1, λ2)]
0.06
0.02
-0.02
-π/4
0
π/4
λ2
0
50
λ1
Im [B121 (λ1, λ2)]
0.06
0.02
-0.02
-π/4
0
π/4
λ2
0
50
λ1

Fig. 2